INSTITUTE OF PHYSICS PUBLISHING PHYSICS IN MEDICINE AND BIOLOGY

Phys. Med. Biol. **47** (2002) 3705–3710 PII: S0031-9155(02)39039-0

Optimization of photoconducting receivers for THz spectroscopy

S R Andrews, A Armitage, P G Huggard[1] and A Hussain

Department of Physics, University of Bath, Bath BA2 7AY, UK

E-mail: s.r.andrews@bath.ac.uk

Received 18 March 2002
Published 17 October 2002
Online at stacks.iop.org/PMB/47/3705

Abstract

We have studied the sensitivity and noise of optically gated dipole receivers made from ion implanted Si and GaAs in an optimized time domain THz spectrometer. The spectrometer uses a room temperature, dc biased, semi-insulating GaAs stripline source capable of generating up to 30 μW average power. The 10% amplitude system bandwidth for 10 μm (50 μm) dipole receivers is 3 THz (1.5 THz). A dynamic range of 4×10^5 Hz$^{-1/2}$ is achieved using a 10 μm dipole GaAs receiver and 2×10^6 Hz$^{-1/2}$ using a 50 μm dipole for a total laser power of 110 mW and THz beam power of 20 μW. The dynamic range achieved with comparable silicon receivers is a factor of 2 smaller.

1. Introduction

Over the last decade the technique of time domain THz spectroscopy (TDTS) has emerged as a powerful tool in the study of numerous areas of science and technology ranging from quantum coherence in semiconductors [1] to imaging of materials [2]. The latter application has attracted particular interest as a potential non-invasive medical probe for diagnosis of skin cancer and burns. The most efficient generation of electromagnetic transients with THz bandwidth is normally achieved by femtosecond excitation of the high electric field regions of biased metal–semiconductor–metal structures [3]. These include various sorts of stripline and antennae with photoconducting feed elements and are usually fabricated on high resistivity bulk GaAs or GaAs deposited by low temperature (LT) molecular beam epitaxy (MBE). The principal sub-picosecond, coherent detection techniques use either photoconductors integrated with microfabricated antennae [4] or electro-optic sampling [5]. The former commonly consists of a dipole antenna bridged by a photoswitch which has a high resistance in the off

[1] Present address: Space Science and Technology Department, Rutherford Appleton Laboratory, Chilton OX11 0QX, UK.

state and a low resistance in the on state. The switch has a turn-on time partly limited by the laser pulse duration (typically ∼100 fs or less) and partly by carrier cooling and a turn-off time which can be engineered to be a few hundred fs by means of ion implantation or LT epitaxial growth. The principle of this device is that THz bandwidth pulse illumination of the antenna only produces a signal current in an external circuit connected to the antenna arms if the photoswitch is simultaneously turned on by an optical gating pulse. Information about the time evolution of the THz electric field can thus be obtained by measuring the current in the external circuit as a function of time delay between the gate pulse and the pulse pumping the THz source. A similar pump-gate approach also allows the electro-optic (EO) effect in crystals such as ZnTe to be used for coherent time domain detection [5]. The photoconducting receiver is generally less affected by laser, mechanical and acoustic noise whilst the EO technique has higher bandwidth and more easily allows parallel signal processing [6].

The first photoconducting receivers were made from ion implanted silicon on sapphire (SOS) [4]. Various materials and methods of construction have since been explored with the aim of improving sensitivity or bandwidth. These include flip-chip bonding of SOS receivers on to lower dispersion Si substrates [7], the epitaxial growth of Si on high resistivity Si substrates with an intervening layer of silicon dioxide [8], the growth of LT GaAs epilayers [9] and GaAs on Si epitaxy [10]. Receiver optimization involves achieving the best compromise between bandwidth, sensitivity and noise in the choice of material, antenna design and optics. In system optimization one must also take into account the THz source and intermediate optics. With the exception of the seminal paper by Van Exter and Grischkowsky [11], the system dynamic range (peak to peak signal amplitude to RMS noise amplitude in unit bandwidth) in photoconducting-type TDTS systems has not previously been discussed in detail. In this paper, we compare receivers made in different materials and describe a few methods for achieving the best system performance.

2. Receiver materials and fabrication

We have studied receivers made from O^+ implanted Si and As^+ implanted GaAs. The Si receivers are of two types. One consists of commercial SOS and has a Si layer 0.6 μm thick. The other consists of 1.1 μm of Si grown by chemical vapour deposition on 0.6 μm of thermal oxide on top of a 1.4 kΩ cm Si substrate. The GaAs receivers consisted of 1 μm of undoped GaAs grown by MBE on a 0.1 μm thick AlAs electrical isolation layer on a semi-insulating GaAs substrate. For each type of receiver a spread of implantation energies (75–500 keV for Si, 0.1–3 MeV for GaAs) was used to obtain a roughly uniform vacancy-depth profile over the thickness of the epilayer. The implant dose and annealing temperature were chosen so as to obtain a good compromise between bandwidth and signal-to-noise ratio. In general, to achieve this one looks for the highest resistivity for a chosen trapping time. The chosen dose was 10^{15} cm^{-2} for all materials. The silicon devices were not annealed whilst the GaAs devices were annealed at 500 ^{o}C for 20 min.

The antenna structures were fabricated in the conventional form [11] of a pair of Ti/Au tabs 20 μm wide and 2.5 μm long with a gap of 5 μm. The tabs were positioned in the middle of a coplanar stripline consisting of two 10 μm wide connection tracks spaced by 10 μm. Ion implantation results in very small Schottky barrier heights so that the tracks need not be annealed. After metallization, the photoconducting layer was stripped away to reveal the underlying insulator except for a 100 μm wide stripe under the dipole arms in order to reduce thermal noise [11].

Table 1. Properties of the photoconducting antennae. The results are based on averaging measurements made on several devices. The relative sensitivity is the peak to peak signal current referred to that in the SOS device. The noise was measured at 7 kHz with a 20 mW. 765 nm gate beam.

Material	Carrier lifetime (fs)	Resistivity (kΩ cm)	Mobility ($cm^2\ V^{-1}\ s^{-1}$)	Relative sensitivity	Illuminated noise ($fA\ Hz^{-1/2}$)
SOS:O^+	430 ± 30	50 ± 5	30 ± 5	1	100 ± 10
Si/oxide:O^+	540 ± 60	20 ± 5	30 ± 5	2 ± 0.2	200 ± 30
GaAs/AlAs:As^+	450 ± 50	50 ± 5	400 ± 50	6 ± 0.3	300 ± 50

3. Bandwidth and sensitivity

Some of the important properties of the receivers are summarized in table 1. The semi-insulating GaAs transmitters used in the characterization were fabricated as conventional coplanar striplines [3] or waveguides with 80 μm or 50 μm gaps, respectively. The 750 nm, 100 fs, 82 MHz repetition rate pump pulse was polarized perpendicular to the tracks [12] and tightly focused at the positive electrode edge to benefit from geometrical and trap enhancement of the bias field [13] and the greater mobility of electrons compared with holes. The pump focus had a $1/e^2$ diameter of $\sim$4 μm $\times$ 100 μm. The line focus is important in maximizing transmitter output without thermal runaway and dielectric breakdown. The carrier lifetimes are in the range 0.4–0.6 ps which leads to the devices all having useful system bandwidth in excess of 3 THz with a peak response near 1 THz. The upper and lower frequencies we have used in defining bandwidth are those where the spectral amplitude has dropped to 10% of maximum. Our results are comparable with the best reported in the literature for Si [7, 8] and LT GaAs [14] receivers with the same dimensions when used with similar sources. This does not represent the ultimate system bandwidth and better results can be obtained (although with lower dynamic range) using an optical rectification source and shorter optical pulses [15].

The absolute power sensitivity of the receivers was measured using a diamond window Golay cell that was calibrated to an accuracy of $\pm$20%. Illuminating the 80 μm gap coplanar stripline transmitter with 170 mW pump power at a dc bias of 60 V yields approximately 30 μW of average THz beam power at room temperature. The SOS receiver had a peak to peak responsivity of 4 $\mu A\ W^{-1/2}$ and that of the others can be deduced using table 1. The Si/oxide receiver is twice as sensitive as that made from SOS because of the greater active layer thickness and more complete absorption of the gate beam. The mobility of the As^+ implanted GaAs is 13 times larger than that of the O^+ implanted Si which accounts for the order of magnitude ratio of their sensitivities at low gate power. At high gate power the GaAs/AlAs receiver is only three times as sensitive because the response is saturated by photocarrier screening of the THz field. Critical in achieving high bandwidth and sensitivity is the alignment of the high resistivity silicon collimating substrate lens relative to the photoconducting gap which must be performed to a precision of order a few tens of μm. The polarization angle of the receiver gate beam should also be set perpendicular to the metal edges of the photoconducting switch to optimize receiver performance. This gives a threefold, gate power independent, increase in signal compared with the orthogonal polarization in which the optical field at the gap edges is reduced by screening currents in the metal [12]. Another important factor is that the off-axis parabolic mirrors that couple radiation between the transmitter and receiver substrate lenses are positioned so as to obtain unity transfer function.

It is notable that there are few reports of μW average THz beam powers from biased transmitters in the literature. Tani *et al* [14] measured 11 μW from a semi-insulating GaAs

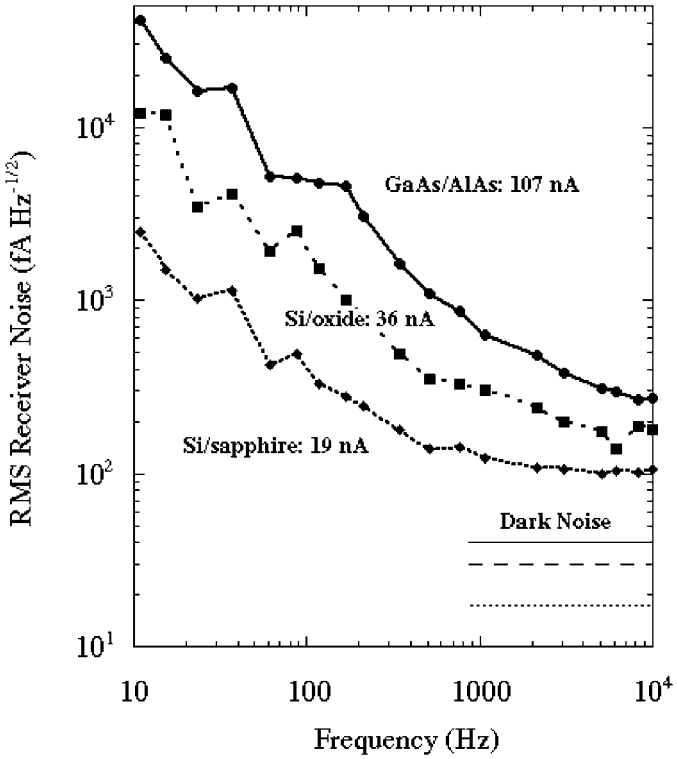

Figure 1. Frequency dependence of current noise for receivers with 20 mW gate power for 10 μm dipole antennae on different materials. Also shown are the peak THz signals and the receiver dark noise. The results are the averages over several devices.

bow tie transmitter and Cai *et al* [16] reported 3 μW using a LT GaAs pointed anode dipole (although there is an error in their calculation). Zhao *et al* [17] recently obtained 40 μW from a thermoelectrically cooled large gap GaAs device, ac biased at several hundred volts. The transmitter bandwidth in these reports appears to be significantly lower than we have achieved. High power THz emission has also recently been reported from unbiased InAs surfaces [18]. The average power in our THz beam is very similar to what we have found in Golay cell measurements of high purity (10^{15} cm^{-3} n-type) InAs at 10 K and in a magnetic field of 5 T when excited with a 1 W pump. Although put forward by other authors as a useful THz source, the latter not only has narrower 10% bandwidth ($\sim$1.5 THz) but is expensive and inconvenient to operate.

4. Dynamic range

Figure 1 shows the noise spectra for various receivers with 20 mW gate power and no THz beam. Below $\sim$1 kHz the dominant contribution to the noise is '$1/f$' noise associated with laser noise and trapping in bulk and surface states. Above $\sim$1 kHz the noise becomes independent of frequency and is mainly made up of contributions from thermal noise associated with the illuminated gap resistance and fluctuations in the dc photocurrent which is present because of the small but finite Schottky barriers either side of the photoconducting gap. Such

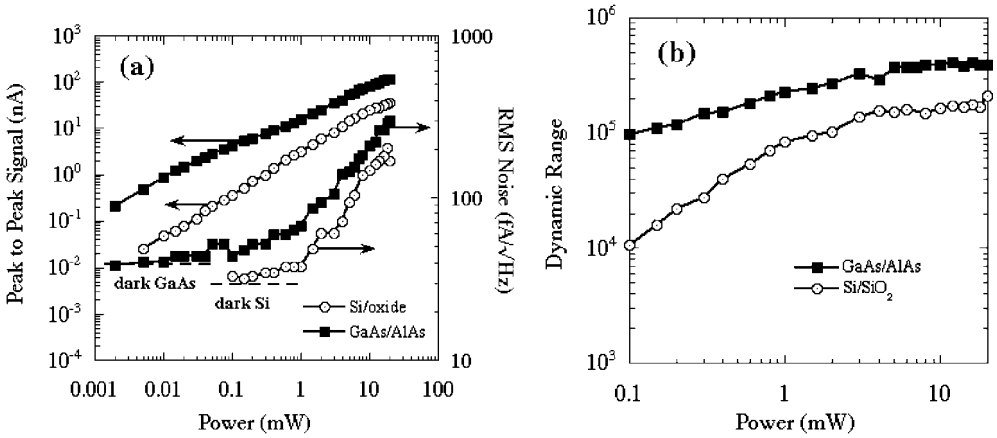

Figure 2. (a) Gate power dependence of receiver signal with average THz beam power of 20 μW and noise at 7 kHz. (b) Gate power dependence of dynamic range obtained from data in (a). The transmitter was a 50 μm gap, coplanar waveguide biased at 40 V and line illuminated with 100 mW pump power.

photocurrents can exceed 10 nA with 20 mW gate power, and fluctuations due to laser noise can then make a significant contribution (>100 fA $Hz^{-1/2}$) to the total. The dark noise is consistent with the combined contributions of thermal noise associated with the gap resistance and current amplifier noise.

Figure 2(a) shows the gate power variation of signal and noise for the Si/oxide and GaAs/AlAs receivers. The frequency of the noise measurements was 7 kHz, which is a convenient modulation frequency when performing synchronous detection. The signal for the Si receiver increases approximately linearly at low power and the GaAs sublinearly at all powers. In both cases the variation becomes more sublinear at high power because of photocarrier screening of the THz electric field. At high gate power the RMS noise varies in proportion to the square root of the gate power which is roughly consistent with contributions from thermal noise arising from the lower illuminated gap resistance and fluctuations in the dc photocurrent (which varies sublinearly with gate power) due to laser power noise. The oxide and AlAs layers under the photoconducting epilayers serve to electrically isolate long lived carriers photo-generated in the underlying, unimplanted material which would otherwise contribute to the thermal noise. Figure 2(b) shows the system dynamic range obtained from the data in figure 2(a). The dynamic range when using the GaAs receiver is 4×10^5 for gate powers >5 mW and the noise equivalent power is 125 aW. The signal currents with 50 μm dipoles are double those discussed above at the expense of halving the bandwidth. With 20 μW average THz beam power a system dynamic range of nearly 2×10^6 and a bandwidth of 1.5 THz is achieved using a 50 μm GaAs dipole receiver.

5. Conclusions

We have studied the sensitivity and noise of optically gated dipole receivers made from ion implanted Si and GaAs in an optimized time domain THz spectrometer. The spectrometer uses a biased semi-insulating GaAs stripline source capable of generating up to 30 μW average power and has a 10% amplitude system bandwidth for 10 μm (50 μm) dipole receivers of 3 (1.5) THz. A dynamic range of 4×10^5 $Hz^{-1/2}$ is achieved using a 10 μm dipole GaAs

receiver and 2×10^6 Hz$^{-1/2}$ using a 50 μm dipole for a total laser power of 110 mW and THz beam power of 20 μW. The dynamic range achieved with comparable silicon receivers is a factor of 2 smaller.

Acknowledgment

We thank the UK Engineering and Physical Science Research Council for financial support.

References

[1] Shah J 1996 *Ultrafast Spectroscopy of Semiconductors and Semiconductor Nanostructures (Springer Series in Solid-State Sciences vol 115)* (Berlin: Springer)
[2] Mittleman D M, Gupta M, Neelamani R, Baraniuk R G, Rudd J V and Koch M 1999 Recent advances in terahertz imaging *Appl. Phys.* B **68** 1085–94
[3] Katzenellenbogen N and Grischkowsky D 1991 Efficient generation of 380 fs pulses of THz radiation by ultrafast laser pulse excitation of a biased metal-semiconductor interface *Appl. Phys. Lett.* **58** 222–5
[4] Smith P R, Auston D H and Nuss M C 1988 Subpicosecond photoconducting dipole antennas *IEEE J. Quantum Electron.* **24** 255
[5] Wu G and Zhang X-C 1996 Ultrafast electro-optic field sensors *Appl. Phys. Lett.* **68** 1604–7
[6] Lu Z G, Campbell P and Zhang X-C 1997 Free-space electro-optic sampling with a high-repetition-rate regenerative amplified laser *Appl. Phys. Lett.* **71** 593–6
[7] Katzenellenbogen N and Grischkowsky D 1993 An ultra-wideband optoelectronic THz beam system *Ultra-Wideband Short-Pulse Electromagnetics* ed H Bertoni *et al* (New York: Plenum) pp 7–20
[8] Katzenellenbogen N, Chan H and Grischkowsky D 1993 Optoelectronic observation of a 65 fs signal feature *QELS Tech. Digest* pp 155–6
[9] Warren A C, Katzenellenbogen N, Grischkowsky D, Woodall J M, Melloch M R and Otsuka N 1991 Subpicosecond, freely propagating electromagnetic pulse generation and detection using GaAs:As epilayers *Appl. Phys. Lett.* **58** 1512–5
[10] Pedersen J E, Keiding S R, Sorensen C B, Lindelof P E, Rühle W W and Zhou X Q 1993 5-THz bandwidth from a GaAs-on-silicon photoconductive receiver *J. Appl. Phys.* **74** 7022
[11] Van Exter M and Grischkowsky D R 1990 Characterization of an optoelectronic terahertz beam system *IEEE Trans. Microw. Theory Tech.* **38** 1684
[12] Huggard P G, Shaw C J, Cluff J A and Andrews S R 1998 Polarization-dependent efficiency of photoconducting THz transmitters and receivers *Appl. Phys. Lett.* **72** 2069–72
[13] Ralph S E and Grischkowsky D 1991 Trap-enhanced electric fields in semi-insulators: the role of electrical and optical carrier injection *Appl. Phys. Lett.* **59** 1972–5
[14] Tani M, Matsuura S, Sakai K and Nakashima S 1997 Emission characteristics of photoconductive antennas based on low-temperature grown GaAs and semi-insulating GaAs *Appl. Opt.* **36** 7853
[15] Kono S, Tani M and Sakai K 2000 Detection of up to 20 THz with a low temperature-grown GaAs photoconductive antenna gated with 15 fs light pulses *Appl. Phys. Lett.* **77** 4104–7
[16] Cai Y, Brener I, Lopata J, Wynn J, Pfeiffer L and Federici J 1997 Design and performance of singular electric field terahetz photoconducting antennas *Appl. Phys. Lett.* **71** 2076–9
[17] Zhao G, Schouten R N, van der Valk N, Wenckebach W Th and Planken P C M 2002 Design and performance of a THz emission setup based on semi-insulating GaAs emitter *Rev. Sci. Instrum.* **73** 1715
[18] Heyman J N, Neocleous P, Hebert D, Cromwell P A, Müller T and Unterrainer K 2001 Terahertz emission from GaAs and InAs in a magnetic field *Phys. Rev.* B **64** 085202